

Mechanisms of Phospholipid Complex Loaded Nanoparticles Enhancing the Oral Bioavailability

Qiang Peng, Zhi-Rong Zhang, Xun Sun, Jiao Zuo, Dong Zhao, and Tao Gong*

Key Laboratory of Drug Targeting and Drug Delivery Systems, Ministry of Education, West China School of Pharmacy, Sichuan University, Southern Renmin Road, No. 17, Section 3, Chengdu 610041, P. R. China

Received November 5, 2009; Revised Manuscript Received January 19, 2010; Accepted February 18, 2010

Abstract: The purpose of the present study was to study the mechanisms of salvianolic acid B phospholipid complex loaded nanoparticles (SalB-PLC-NPs) enhancing the oral bioavailability of SalB by in situ perfusion model in rats and to evaluate the potential of phospholipid complex loaded nanoparticles (PLC-NPs) serving as an efficient oral delivery system to enhance the bioavailability of highly water-soluble drugs. SalB-PLC-NPs, prepared by a solvent evaporation method, exhibited a spherical shape with a mean particle size and a zeta potential of 112.2 nm and -44.2 mV, respectively. The drug entrapment efficiency and drug loading were 86.19% and 3.21%, respectively. The lyophilized SalB-PLC-NPs, prepared with 10% maltose as the cryoprotectant, presented sustained release profiles in artificial gastric juice (0.1 M HCl with pH 1.2) and intestinal juice (PBS with pH 6.8 and 7.4). The absorption mechanisms were studied using a modified in situ perfusion method in rats, which showed the segment dependent absorption characteristics of SalB, SalB-PLC as well as SalB-PLC-NPs. The greatest absorption was obtained when SalB-PLC-NPs were perfused in colon. The possibility of intestinal lymphatic transport of SalB-PLC-NPs was investigated using mesenteric lymph vessel cannulation. Microscope (fluorescence and natural light) observation of lymph indicated that nanoparticles underwent intestinal lymphatic transport. In conclusion, the enhanced oral bioavailability of SalB was contributed to both the PLC and NPs. Importantly, our studies indicate that PLC-NPs may be a promising delivery system to enhance the oral bioavailability of highly water-soluble drugs.

Keywords: Phospholipid complex; nanoparticles; single pass intestinal perfusion; oral delivery; lymphatic transport

Introduction

One of the most important factors affecting the bioavailability of an orally administered drug is its intestinal permeability,¹ which is usually used to indicate the in vivo absorption rate and extent of orally administered drugs.² Therefore, studies on drug permeation across the intestinal

epithelium are necessary for drug research and development as well as for the research of basic absorption mechanisms.

There are several typical methods for evaluating the intestinal permeability of oral drugs, including (1) in situ intestinal perfusion studies in a suitable animal model (most commonly rats); (2) diffusion studies with intestinal segments from various animals (e.g., rats and rabbits) or monolayers of suitable epithelial cells (e.g., Caco-2 cells); (3) uptake studies in brush-border membrane vesicles prepared from

* Corresponding author. Mailing address: Sichuan University, Southern Renmin Road, No. 17, Section 3, Chengdu 610041, P. R. China. Tel: +86 28 85501615. Fax: +86 28 85501615. E-mail: gongtaoy@126.com.

(1) Grassi, M.; Cadelli, G. Theoretical considerations on the in vivo intestinal permeability determination by means of the single pass and recirculating techniques. *Int. J. Pharm.* **2008**, *229*, 95–105.

(2) Dahan, A.; West, B. T.; Amidon, G. L. Segmental-dependent membrane permeability along the intestine following oral drug administration: Evaluation of triple single pass intestinal perfusion (TSPIP) approach in the rat. *Eur. J. Pharm. Sci.* **2009**, *36*, 320–329.

intestinal segments.^{3–5} Among these methods, the single pass intestinal perfusion (SPIP) approach in rats is the most frequently used technique for studies of drug absorption.^{2,5–12} The SPIP method has been shown to provide predictive values for in vivo absorption in humans.^{13,14} In addition, the SPIP technique provides the unique advantages of experimental control of drug concentration, intestinal perfusion rate and the length of perfused intestine, as well as ability to study different intestinal segments, without affecting the intestinal blood supply. Hence, the SPIP model, which measures the loss of compound in the perfusate, has been listed in the FDA guidance as a permeability classification tool for the characterization of a drug according to the Biopharmaceutics Classification System (BCS).¹⁵

Phospholipid complex, which is formed usually in a nonaqueous solvent, has been studied for many years to enhance the therapeutic efficacy of some drugs with poor

oral absorption.^{16–19} In recent years, the oral bioavailability of many drugs has been enhanced by the approach of forming drug–phospholipid complex.^{20–22} In the previous study, our group prepared the salvianolic acid B–phospholipid complex and entrapped the complex in nanoparticles. After oral administration of the phospholipid complex loaded nanoparticles in rats, the bioavailability of salvianolic acid B was significantly enhanced,²³ which was consistent with the results reported by Cui et al.²⁴

Although the result of our previous work was encouraging, it is still unknown whether it is the complex or nanoparticles or both that contribute to the enhanced bioavailability of salvianolic acid B. Therefore, the main aim of this present work was using the modified SPIP technique in male Sprague–Dawley rats to compare the permeability and absorption rate among salvianolic acid B (SalB), salvianolic acid B–phospholipid complex (SalB-PLC) and salvianolic acid B–phospholipid complex loaded nanoparticles (SalB-PLC-NPs) in different sites (i.e., stomach, duodenum, jejunum, ileum and colon) and to study the mechanisms of SalB-PLC-NPs enhancing the oral bioavailability of SalB, to investigate the possibility of lymphatic transport of SalB-PLC-NPs, and to evaluate the potential of PLC-NPs serving as an effective oral delivery system for highly water-soluble drugs. Initially, SalB-PLC-NPs were prepared by a solvent evaporation method. Then, the physicochemical characteristics and in vitro release behavior of SalB-PLC-NPs were investigated. The absorption characteristics of SalB, SalB-PLC and SalB-PLC-NPs in different sites in GIT were studied and compared to understand why SalB-PLC-NPs

- (3) Hidalgo, I.; Raub, T.; Borchardt, R. Characterization of the human colon carcinoma cell line (Caco-2) as a model system for intestinal epithelial permeability. *Gastroenterology* **1989**, *96*, 736–749.
- (4) Artursson, P.; Karlsson, J. Correlation between oral drug absorption in humans and apparent drug permeability coefficients in human intestinal epithelial (Caco-2) cells. *Biochem. Biophys. Res. Commun.* **1991**, *175*, 880–885.
- (5) Li, H. L.; Zhao, X. B.; et al. Enhancement of gastrointestinal absorption of quercetin by solid lipid nanoparticles. *J. Controlled Release* **2009**, *133*, 238–244.
- (6) Schanker, L. S.; Tocco, D. J.; et al. Absorption of drugs from the rat small intestine. *J. Pharmacol. Exp. Ther.* **1958**, *123*, 81–88.
- (7) Barr, W. H.; Riegelman, S. Intestinal drug absorption and metabolism I: comparison of methods and models to study physiological factors of in vivo and in vitro intestinal absorption. *J. Pharm. Sci.* **1970**, *59*, 154–163.
- (8) Schurgers, N.; Bijdendijk, J.; et al. Comparison of four experimental techniques for studying drug absorption kinetics in the anesthetized rat in situ. *J. Pharm. Sci.* **1986**, *75*, 117–119.
- (9) Venkatesh, G.; Ramanathan, S.; et al. Permeability of atenolol and propranolol in the presence of dimethyl sulfoxide in rat single pass intestinal perfusion assay with liquid chromatography/UV detection. *Biomed. Chromatogr.* **2007**, *21*, 484–490.
- (10) Zakeri-Milani, P.; Valizadeh, H.; et al. Predicting human intestinal permeability using single-pass intestinal perfusion in rat. *J. Pharm. Pharm. Sci.* **2007**, *10*, 368–379.
- (11) Ho, Y. F.; Lai, M. Y.; et al. Application of rat in situ single-pass intestinal perfusion in the evaluation of presystemic extraction of indinavir under different perfusion rates. *J. Formosan Med. Assoc.* **2008**, *107*, 37–45.
- (12) Richter, M.; Gyémánt, N.; et al. Comparative effects on intestinal absorption in situ by p-glycoprotein-modifying HIV protease inhibitors. *Pharm. Res.* **2004**, *21*, 1862–1866.
- (13) Kim, J. S.; Mitchell, S.; et al. The suitability of an in situ perfusion model for permeability determinations: utility for BCS class/biowaiver requests. *Mol. Pharmaceutics* **2006**, *3*, 686–694.
- (14) Lennernas, H. Animal data: the contributions of the Ussing Chamber and perfusion systems to predicting human oral drug delivery in vivo. *Adv. Drug Delivery Rev.* **2007**, *59*, 1103–1120.
- (15) Center for Drug Evaluation and Research (CDER). *Waiver of in vivo bioavailability and bioequivalence studies for immediate release dosage forms containing certain active moieties/active ingredients based on a biopharmaceutical classification system*; American Food and Drug Administration (FDA): 1999.
- (16) Carini, R.; Comoglio, A.; et al. Lipid peroxidation and irreversible damage in the rat hepatocyte model: protection by the silybin-phospholipid complex IdB 1016. *Biochem. Pharmacol.* **1992**, *43*, 2111–2115.
- (17) Conti, M.; Malandrino, S.; Magistretti, M. J. Protective activity of silybin-phosphatidylcholine complex on liver damage in rodents. *Jpn. J. Pharmacol.* **1992**, *60*, 315–321.
- (18) Morazzoni, P.; Montalbetti, A.; et al. Comparative pharmacokinetics of silybin-phosphatidylcholine complex and silymarin in rats. *Eur. J. Drug Metab. Pharmacokinet.* **1993**, *18*, 289–297.
- (19) Comoglio, A.; Tomasi, A.; et al. Scavenging effect of silybin, a new silybin-phospholipid complex, on ethanol-derived free radicals. *Biochem. Pharmacol.* **1995**, *50*, 1313–1316.
- (20) Maiti, K.; Mukherjee, K.; et al. Enhanced therapeutic benefit of quercetin-phospholipid complex in carbon tetrachloride induced acute liver injury in rats: a comparative study. *Iran J. Pharmacol. Ther.* **2005**, *4*, 84–90.
- (21) Xiao, Y. Y.; Song, Y. M.; et al. The preparation of silybin-phospholipid complex and the study on its pharmacokinetics in rats. *Int. J. Pharm.* **2006**, *307*, 77–82.
- (22) Maiti, K.; Mukherjee, K.; et al. Curcumin-phospholipid complex: Preparation, therapeutic evaluation and pharmacokinetic study in rats. *Int. J. Pharm.* **2007**, *330*, 155–163.
- (23) Peng, Q.; Gong, T.; Zuo, J.; et al. Enhanced oral bioavailability of salvianolic acid B by phospholipid complex loaded nanoparticles. *Pharmazie* **2008**, *63*, 661–666.
- (24) Cui, F. D.; Shi, K.; Zhang, L. Q.; et al. Biodegradable nanoparticles loaded with insulin-phospholipid complex for oral delivery: preparation, in vitro characterization and in vivo evaluation. *J. Controlled Release* **2006**, *114*, 242–250.

could enhance the oral bioavailability of SalB. Finally, in order to study whether nanoparticles are transported via lymph, a red fluorescence dye DiI (1,1'-dioctadecyl-3,3',3'-tetramethylindocarbocyanine perchlorate) was incorporated into nanoparticles and mesenteric lymph vessel cannulation was performed.

Experimental Section

Materials. Phospholipid (soybean lecithin, with phosphatidylcholine (PC) content of 70%–97%) was purchased from Shanghai Tai-wei Pharmaceutical Co. Ltd. (Shanghai, China). Salvianolic acid B (SalB) was extracted by us, with a purity of 88.18%. SalB standard (purity higher than 98%) was provided by Zhongxin Innova Laboratories (Tianjin, China). Salvianolic acid B–phospholipid complex (SalB-PLC) was completely formed according to our previous method.²³ Poloxamer188 (F68) was provided by Nanjing Well Chemical Co., Ltd. (Nanjing, China). DiI was purchased from Beyotime Institute of Biotechnology (Jiangsu, China). All other chemical reagents were of analytical grade or better.

Preparation of SalB-PLC-NPs. SalB-PLC-NPs were prepared based on our previous study²³ with some modifications. Initially, at a ratio of 1:1 (w/w), SalB-PLC and phospholipid were codissolved in 1 mL of absolute ethanol as the organic phase. Under high speed magnetic stirring the above-mentioned organic solution was quickly injected into an aqueous solution that contained 1.0% of F68 (w/v). Then the suspension was evaporated to one-fourth of the initial volume under vacuum at 45 °C so that the organic solvent could be completely removed. After dilution to 10 mL with double distilled water, the suspension was processed with high pressure homogenization for 5 cycles.

Physicochemical Characterization of SalB-PLC-NPs. The mean particle size and zeta potential of SalB-PLC-NPs were determined by dynamic light scattering (DLS) and electrophoretic light scattering (ELS) respectively, using a Zetasizer Nano ZS90 instrument (Malvern Instruments Ltd., U.K.). Briefly, 0.1 mL of the above produced suspension was diluted to 1 mL with distilled water for measuring particle size, and another 1 mL of the initial suspension was taken for the determination of zeta potential without dilution. The diluted and undiluted suspension was added into the corresponding sample cell, which was inserted into the instrument for measurement of particle size and zeta potential, respectively. Some important measurement conditions were as follows: dispersant, water; temperature, 25 °C; cycles of measurement, automatically determined by the instrument system. The particle size data were evaluated using the intensity distribution. All the measurements were performed in triplicate.

The morphology of SalB-PLC-NPs was observed using a scanning electron microscope (SEM, JSM-5900 LV, JEOL, Japan) at an accelerating voltage of 20 kV. One drop of SalB-PLC-NPs suspension was placed on a graphite surface. After dryness, the sample was coated with gold using an Ion Sputter.

Entrapment Efficiency and Drug Loading. The amount of drug entrapped in nanoparticles was determined indirectly according to the traditional centrifugation method^{25,26} with some modifications. Briefly, after the surface charge of SalB-PLC-NPs was neutralized by adding 0.1 M HCl, a certain volume of the suspension was accurately taken and dissolved in absolute ethanol by sonication. The total amount of drug was obtained by measuring the above-mentioned solution with HPLC. A same volume of the neutralized suspension was accurately taken and centrifuged at 14,000 rpm for 30 min at 4 °C using Allegra X-22R Centrifuge (Beckman-Coulter). The precipitate was dissolved in absolute ethanol by sonication and determined under the same condition, and the amount of drug entrapped in nanoparticles was gained. The entrapment efficiency (EE) and drug loading (DL) were calculated by the following equations.²⁷ All the determinations were performed in triplicate.

$$EE = W_s/W_{total} \times 100\%$$

$$DL = W_s/W_{lipid} \times 100\%$$

W_s : amount of drug entrapped in SalB-PLC-NPs (equivalent to the amount of SalB). W_{total} : amount of drug added (equivalent to the amount of SalB). W_{lipid} : amount of drug added plus material added.

Preparation and Evaluation of the Lyophilized SalB-PLC-NPs. The lyophilized SalB-PLC-NPs were prepared as follows: SalB-PLC-NPs were dispersed in a solution containing 10% (w/v) maltose as the cryoprotectant. The resulting solution was frozen at –50 °C overnight and then lyophilized for 24 h using a freeze drier (ThermoSavant ModulyoD-230, Thermo Electron). The lyophilized powder was obtained and kept sealed in a desiccator at room temperature.

The lyophilized SalB-PLC-NPs were reconstituted with double distilled water, of which the particle size, zeta potential and entrapment efficiency were determined according to the method described above and compared with those before lyophilization. In addition, the particle size, PDI and zeta potential of lyophilized products reconstituted in 0.1 M HCl and PBS (pH 6.8 and 7.4) were measured. Finally, stability of the lyophilized products within 3 months was investigated. All the determinations were carried out in triplicate.

In Vitro Release Studies. In vitro drug release from SalB-PLC-NPs was performed in artificial gastric juice (0.1 M HCl with pH 1.2) and intestinal juice (phosphate buffer

(25) Hu, F. Q.; Yuan, H.; et al. Preparation of solid lipid nanoparticles with clobetasol propionate by a novel solvent diffusion method in aqueous system and physicochemical characterization. *Int. J. Pharm.* **2002**, *239*, 121–128.

(26) Peng, H. S.; Liu, X. J.; et al. Voriconazole into PLGA nanoparticles: Improving agglomeration and antifungal efficacy. *Int. J. Pharm.* **2008**, *352*, 29–35.

(27) Luo, Y. F.; Chen, D. W.; et al. Solid lipid nanoparticles for enhancing vinpocetine's oral bioavailability. *J. Controlled Release* **2006**, *114*, 53–59.

solution (PBS) with pH 6.8 and 7.4) without enzymes, using the dialysis bag method.²⁷ The dialysis bags with a molecular weight cutoff of 8000–14000 were used to detain SalB-PLC-NPs and allow the free drug to disperse into the dissolution media. The dialysis bags were soaked in double distilled water for 12 h before use. The lyophilized products were redispersed in double distilled water, and 1 mL of SalB-PLC-NPs suspension was added to the bags, which were tightly bundled at the two ends. The bags were placed in antibiotic bottles (capacity: 10 mL), and 4 mL of the dissolution media was added. The antibiotic bottles were shaken in a horizontal shaker (Shenzhen worldwide industry, Co. Ltd., China) at 60 rpm, 37 ± 1 °C. At predetermined time intervals, the dissolution media in the antibiotic bottles were completely withdrawn and fresh media were added to maintain the sink condition. The amount of drug released from nanoparticles was analyzed using HPLC. All the operations were carried out in triplicate.

Gastrointestinal Absorption in Situ. Healthy male Sprague–Dawley rats (210–280 g) for GI absorption studies were purchased from Laboratory Animal Center of Sichuan University (Chengdu, P. R. China). All animal experiments were approved by the Institutional Animal Care and Use Committee of Sichuan University. Prior to use, rats were acclimatized for at least 7 days. They were housed in cages (5 rats per cage) under controlled conditions (25 °C, 55% air humidity) with free access to water and standard rat chow.

Stomach Absorption Studies. The procedure for the in situ stomach absorption studies was conducted according to a published method.^{5,28} Five healthy SD rats were fasted overnight before studies with free access to water only. Anesthesia was performed with 1% sodium pentobarbital (40 mg/kg body weight) by intraperitoneal administration. Then the anesthetized rats were constrained in a supine position and placed under infrared lamps to maintain body temperature at 37 °C. The abdomen was opened with a 3 cm long midline longitudinal incision. The pylorus of stomach was cannulated with glass tubing (2 mm, i.d.). A small incision was made in cardia, then the stomach was rinsed with simulated gastric media. Then the pylorus and cardia were both ligated with surgical silk suture. The studied drugs (SalB, SalB-PLC and the lyophilized SalB-PLC-NPs) were dissolved or dispersed in artificial gastric juice at the same drug concentration of 300 $\mu\text{g}/\text{mL}$ (equivalent to SalB). 4 mL of the above-mentioned drug solution was injected into stomach of individual rat using injection syringe, and the stomach was put back into the abdomen which was covered with a piece of sterilized absorbent gauze wetted with normal saline solution. After 2 h the solution remaining in the stomach was collected and combined with a certain volume of artificial gastric juice which was used to rinse the stomach twice. Then, the mixed solution was diluted to 25 mL, 1.5 mL of which was centrifuged at 6,000 rpm for 10 min, and

1 mL of the supernatant was sonicated and diluted in absolute ethanol. A 10 μL aliquot of the resultant solution was injected into HPLC.

Single Pass Intestinal Perfusion Studies. The in situ single pass perfusion studies were performed according to the methods described previously,^{2,13,29} but with some modifications. The methods of simultaneous perfusion in two segments were utilized to reduce the number of rats used in the experiment. Briefly, SD rats were fasted overnight before experiments with free access to water only. The predisposal treatment of rats was the same as above. When the abdomen was opened, 10 cm long duodenum (1 cm distal to pyloric sphincter) and ileum (20 cm proximal to cecum) of each rat were simultaneously exposed and cannulated at both ends with glass tubing. The bile duct was ligated to eliminate the influence of bile. Care was taken to minimize the surgery and maintain an intact blood circulation. The selected segments were rinsed with 37 °C physiological saline solution, and then attached to the perfusion assembly consisting of a peristaltic pump (BT00-100M, Baoding Longer Precision Pump Co. Ltd., China), and covered with a piece of sterilized absorbent gauze wetted with 37 °C normal saline solution. Before perfusing drugs, the selected segments were equilibrated with Krebs–Ringer perfusate solution (7.8 g of NaCl, 0.35 g of KCl, 1.37 g of NaHCO_3 , 0.02 g of MgCl, 0.22 g of NaH_2PO_4 and 1.48 g of glucose in 1000 mL of distilled water) at a flow rate of 0.4 mL/min for 15 min, and then the perfusate solution was emptied. The studied drugs (SalB, SalB-PLC and the lyophilized SalB-PLC-NPs), dissolved or dispersed in 15 mL of Krebs–Rings perfusate solution with drug concentration of 300 $\mu\text{g}/\text{mL}$ (equivalent to SalB), were perfused through the segments at a flow rate of 0.2 mL/min for 1 h. At the end of the experiment, the remaining perfusate solution was collected and combined with a certain volume of the Krebs–Ringer perfusate solution which was used to rinse the segments twice. Then, the mixed solution was diluted to 25 mL, 1.5 mL of which was centrifuged at 6,000 rpm for 10 min, and 1 mL of the supernatant was sonicated and diluted in absolute ethanol. A 10 μL aliquot of the resultant solution was injected into HPLC. In addition, the length and inner diameter of selected segments were measured.

In another group of rats, about 10 cm long jejunum (15 cm to pyloric sphincter) and colon (2 cm distal to cecum) of each rat were cannulated and perfused as the same method described above. Each drug was studied following its simultaneous perfusion through every segment in five rats.

The absorption rate constant (K_a) and apparent permeability coefficients (P_{app}) were calculated using the following equations:

$$K_a = (X_0 - X_t) / C_0 t V$$

(28) Barthe, L.; Woodley, J.; Houin, G. Gastrointestinal absorption of drugs: methods and studies. *Fundam. Clin. Pharmacol.* **1999**, *133*, 154–168.

(29) Fagerholm, U.; Johansson, M.; Lennernas, H. Comparison between permeability coefficients in rat and human jejunum. *Pharm. Res.* **1996**, *13*, 1336–1342.

$$P_{app} = Q \cdot \ln(X_{in}/X_{out}) / 2\pi r l$$

where X_0 was the total amount of drug in the perfusate solution at 0 h, X_t was the total amount of drug in the remaining perfusate at the end of the experiment, C_0 was the drug concentration at 0 h, t was the perfusion time, V was the volume of the perfused intestine segment; Q was the flow rate, X_{in} and X_{out} were the inlet and outlet drug amount, and r and l were the radius and length of the perfused intestinal segment.

Preparation and Absorption of Fluorescent Nanoparticles (DiI-SalB-PLC-NPs). DiI-SalB-PLC-NPs were prepared as described in the section of Preparation of SalB-PLC-NPs, with SalB-PLC and phospholipid as well as DiI being collectively dissolved in absolute ethanol.

The absorption studies of DiI-SalB-PLC-NPs were performed as follows: The predisposal treatment of rats was the same as above. After opening the abdomen of rats, about 10 cm long segments of duodenum, jejunum, ileum and colon (only one segment per rat) were washed and ligated at two ends, respectively. The bile duct of each rat was also ligated. 1 mL of DiI-SalB-PLC-NPs suspension was injected into the selected intestinal segments. After 1 h, mesenteric lymph duct cannulation was performed to collect lymph fluid for observation under microscope (fluorescence and natural light. Axiovert 40 CFL, Carl Zeiss, Germany).

The mesenteric lymph duct cannulation was performed according to the methods reported previously.^{30–32} Briefly, a midline incision was made and the mesenteric lymphatic vessel was exposed (adjacent to the superior mesenteric artery) by reflecting the loops of intestine to the left of rat body, and isolated by blunt dissection. The lymphatic duct was cannulated by self-made tubing with visible flow of lymph.

HPLC Analysis. All quantifications were performed by an HPLC system consisting of a Waters 2690 separation module and a 996 photodiode array (PDA) detector; and data were collected and processed using Millennium software version 3.2 (Waters, Milford, MA). The stationary phase, Diamonsil C₁₈ column (200 mm × 4.6 mm, 5 μm), was kept at 35 °C. The mobile phase consisting of acetonitrile, methanol, and 0.1% phosphoric acid at a ratio of 25:10:65 was freshly prepared, filtered through a 0.22 μm membrane filter before use and degassed via an online degasser. The flow rate was 1.0 mL/min, and a wavelength of 286 nm was used for detection. The HPLC assay was linear in the range of 1–400 μg/mL ($r = 0.9999$) with a limit of detection

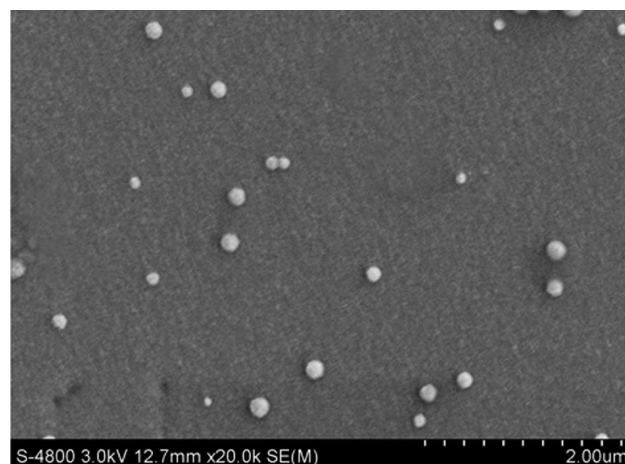


Figure 1. Scanning electron micrograph of SalB-PLC-NPs; scale bar: 0.2 μm.

(LOD) of 100 ng/mL. The mean recoveries of high, middle and low concentrations were 99.47%, 99.31% and 98.22%, respectively.

Statistical Analysis. All data were analyzed using the Student's *t*-test with the *p* value less than 0.05 as the minimal level of significance.

Results

Preparation and Physicochemical Characterization of SalB-PLC-NPs. SalB-PLC-NPs, prepared by the solvent evaporation method, were a clear suspension with light blue opalescence. The mean particle size, polydispersity index (PDI) and zeta potential of SalB-PLC-NPs were 112.2 ± 1.5 nm, 0.163 ± 0.024 and -44.2 ± 0.7 mV, respectively ($n = 3$).

The morphology of SalB-PLC-NPs was observed by SEM, and the image (Figure 1) showed SalB-PLC-NPs were regularly spherical in shape and the particle size was consistent with that determined by DLS.

The entrapment efficiency and drug loading of SalB-PLC-NPs, as determined by the modified ultracentrifugation method, were $86.19 \pm 1.72\%$ and $3.21 \pm 0.04\%$, respectively ($n = 3$).

Preparation and Evaluation of the Lyophilized SalB-PLC-NPs. After lyophilization a porous white powder was obtained. The products could be quickly reconstituted in double distilled water and form a steady suspension. As seen in Table 1, the values of mean particle size, PDI and zeta potential of lyophilized SalB-PLC-NPs were a little lower than those before lyophilization, and the entrapment efficiency of lyophilized SalB-PLC-NPs was a little higher. Generally, however, the physicochemical properties of SalB-PLC-NPs did not essentially change after lyophilization. The results shown in Table 2 indicate that the mean size, PDI and zeta potential of lyophilized SalB-PLC-NPs in PBS (pH 6.8 and 7.4) are almost the same as those in water (see Table 1 “after lyophilization”). When 0.1 M HCl served as the medium, however, the mean size increased, and the zeta potential inverted to

- (30) Deitch, E. A.; Adams, C.; et al. A time course study of the protective effect of mesenteric lymph duct ligation on hemorrhagic shock-induced pulmonary injury and the toxic effects of lymph from shocked rats on endothelial cell monolayer permeability. *Surgery* **2001**, *129*, 39–47.
- (31) Jordan, J. R.; Moore, E. E.; et al. Gelsolin is depleted in post-shock mesenteric lymph. *J. Surg. Res.* **2007**, *143*, 130–135.
- (32) Peltz, E. D.; Moore, E. E.; et al. Proteome and system ontology of hemorrhagic shock: exploring early constitutive changes in postshock mesenteric lymph. *Surgery* **2009**, *146*, 347–357.

Table 1. The Mean Size, PDI, Zeta Potential and Entrapment Efficiency of SalB-PLC-NPs, before and after Lyophilization (Water Served as Medium)^a

sample	mean size (nm)	PDI	zeta potential (mV)	entrapment efficiency (%)
before lyophilization	106.3 ± 1.6	0.159 ± 0.020	-44.3 ± 0.8	87.34 ± 1.85
after lyophilization	103.5 ± 1.8	0.150 ± 0.023	-43.6 ± 1.1	87.59 ± 1.91

^a Values are mean ± SD, *n* = 3.

Table 2. The Mean Size, PDI and Zeta Potential of Lyophilized SalB-PLC-NPs in Different Media^a

medium	mean size (nm)	PDI	zeta potential (mV)
0.1 M HCl	136.7 ± 3.2	0.161 ± 0.029	11.91 ± 0.6
PBS (pH 6.8)	103.3 ± 1.7	0.156 ± 0.031	-42.8 ± 1.2
PBS (pH 7.4)	103.2 ± 1.6	0.154 ± 0.028	-42.9 ± 1.2

^a Values are mean ± SD, *n* = 3.

Table 3. Stability of Lyophilized SalB-PLC-NPs within 3 Months^a

T (month)	mean size (nm)	PDI	zeta potential (mV)	EE (%)
0	103.5 ± 1.8	0.150 ± 0.023	-43.6 ± 1.1	87.59 ± 1.91
1	103.9 ± 1.7	0.147 ± 0.024	-43.4 ± 1.3	86.93 ± 1.87
2	104.3 ± 1.9	0.155 ± 0.028	-42.2 ± 1.4	86.16 ± 1.96
3	107.8 ± 2.3	0.162 ± 0.030	-42.7 ± 1.3	85.71 ± 2.03

^a Values are mean ± SD, *n* = 3.

positive charge with lower values. In addition, Table 3 shows that there was no significant change in the stability of lyophilized products within 3 months.

In Vitro Release Studies. The drug release profile from SalB-PLC-NPs by dynamic dialysis method is shown in Figure 2. During the initial stage the drug release rate in all the three dissolution media was conspicuously fast. In contrast, after the initial stage the release rate became very slow. Hence, the release profile could be divided into two sections: the first part was the initial burst release phase, and the second one was called the sustained release phase. In the initial burst release phase (the first 8 h) about 30.49%, 66.59% and 71.24% of drug (equivalent to SalB)

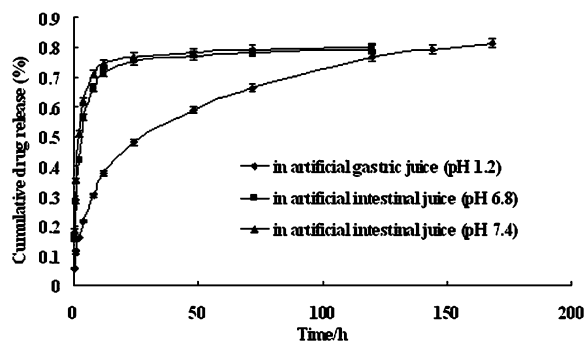


Figure 2. In vitro release profile of lyophilized SalB-PLC-NPs in artificial gastric juice (0.1 M HCl with pH 1.2) and artificial intestinal juice (PBS with pH 6.8 and 7.4). Each data presented as mean ± SD (*n* = 3).

were released into artificial gastric juice (pH 1.2) and intestinal juice (pH 6.8 and 7.4), respectively. In the second phase drug release in artificial gastric juice and two kinds of intestinal juice lasted for 168 h and 120 h, respectively, and displayed a noticeable sustained release property. In addition, Figure 2 also shows that the drug release rate in artificial intestinal juice was much faster than that in gastric juice, and the release rate in intestinal juice with higher pH value was a little faster than in intestinal juice with lower pH value, especially in the initial burst release phase.

The drug release in artificial gastric juice was fitted to Higuchi and Weibull models, with regression equations as follows: $Q = 0.0605t^{0.5} + 0.1041$ ($R^2 = 0.9573$) and $\text{Ln Ln}(1/(1 - Q)) = 0.5417t - 2.1965$ ($R^2 = 0.9931$), respectively. However, the drug release in intestinal juice with pH of 6.8 was only somewhat fitted to Weibull model and regression equation was $\text{Ln Ln}(1/(1 - Q)) = 0.3779t - 1.0085$ ($R^2 = 0.8559$), and the drug release in intestinal juice with pH of 7.4 was a little fitted to Peppas model with regression equation of $\text{Ln } Q = 0.2208 \text{ Ln } t - 1.0347$ ($R^2 = 0.7356$).

Stomach Absorption Studies. It was well-known that the stomach was not a good site for oral drug absorption. In accordance with this, the data showed that stomach absorption was low not only for drug in molecular state but also for nanoparticles. The absorption percentages of SalB, SalB-PLC and SalB-PLC-NPs in the stomach were only 4.78 ± 1.45%, 7.29 ± 1.46% and 8.03 ± 2.04%, respectively (*n* = 5).

Single Pass Intestinal Perfusion Studies. In the present work, absorption characteristics of SalB, SalB-PLC and SalB-PLC-NPs in four different intestinal segments (duodenum, jejunum, ileum and colon) were studied. Comparison among four different intestinal segments of the absorption rate constant (K_a) and apparent permeability coefficients (P_{app}) obtained by in situ perfusion in SPIP model are presented in Figure 3 and Figure 4, respectively. It is interesting to notice that not only for SalB but also for SalB-PLC and SalB-PLC-NPs, the values of both K_a and P_{app} appeared to be significantly higher in ileum and colon than those in duodenum and jejunum (** $P < 0.01$; *** $P < 0.001$). For the three drugs individually, no significant difference of absorption was observed between duodenum and jejunum, but the values of K_a and P_{app} were substantially higher in colon than those in ileum (** $P < 0.01$; *** $P < 0.001$).

Comparison of K_a and P_{app} among these three drugs obtained by in situ perfusion in SPIP model is described in

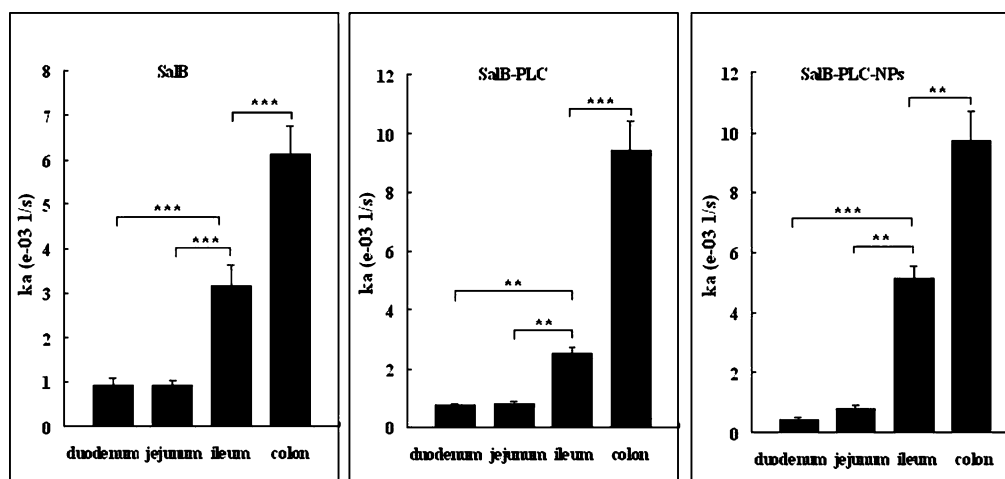


Figure 3. The absorption rate constant (K_a) obtained by in situ perfusion in SPIP model, comparison among four different intestinal segments. Data presented as mean \pm SD ($n = 5$). ** $P < 0.01$; *** $P < 0.001$.

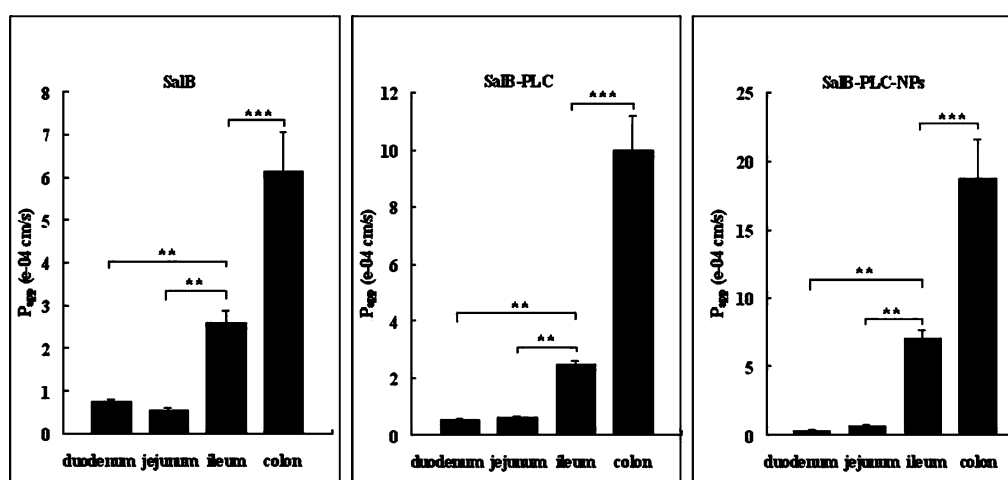


Figure 4. The apparent permeability coefficients (P_{app}) obtained by in situ perfusion in SPIP model, comparison among four different intestinal segments. Data presented as mean \pm SD ($n = 5$). ** $P < 0.01$; *** $P < 0.001$.

Figure 5 and Figure 6. The data showed that there was no significant difference for both K_a and P_{app} in duodenum among these three drugs, and the same results were observed in jejunum. In ileum, however, SalB-PLC-NPs presented higher K_a and P_{app} values than the other two drugs (* $P < 0.05$; ** $P < 0.01$), but there was no significant difference between SalB and SalB-PLC. In colon SalB-PLC and SalB-PLC-NPs showed higher K_a values than SalB (* $P < 0.05$), but there was no significant difference between SalB-PLC and SalB-PLC-NPs. Meanwhile, SalB-PLC-NPs displayed higher P_{app} values in colon than the other two drugs (*** $P < 0.001$), and SalB-PLC showed higher P_{app} values than SalB (** $P < 0.01$). These results indicated that the absorption of SalB-PLC-NPs in ileum and colon was significantly better than the other two drugs, and SalB-PLC showed better absorption in colon than SalB. The best two sites for SalB-PLC-NPs absorption were ileum ($K_a = 5.14 \pm 0.42 \times 10^{-3}$; $P_{app} = 7.04 \pm 0.62 \times 10^{-4}$) and colon ($K_a = 9.70 \pm 1.02 \times 10^{-3}$; $P_{app} = 1.87 \pm 0.29 \times 10^{-3}$).

Preparation and Absorption of Fluorescent Nanoparticles (DiI-SalB-PLC-NPs). In order to study whether nanoparticles were transported via lymph, fluores-

cent nanoparticles (DiI-SalB-PLC-NPs) were prepared and mesenteric lymph vessel cannulation was performed.

Fluorescence images of lymph are shown in Figure 7. The fluorescence spot could be clearly seen in lymph sample taken after administration in colon (Figure 7E), and the weaker fluorescence could be observed in lymph sample taken after administration in ileum. In contrast, no fluorescent signal was detected in blank lymph or the lymph sample collected after administration in duodenum or jejunum. Micrographs of lymph observed under natural light are shown in Figure 8. Only a few particles were observed in blank lymph (Figure 8A), while a large number of particles appeared in lymph after administration of nanoparticles in any segment (Figure 8B–D) and much more when administered in colon (Figure 8E).

Discussion

Usually, in the preparation of nanoparticles it is required to add another matrix besides phospholipid to enhance the stability of nanoparticles. In our studies, however, only soybean lecithin was used as vehicle material. After complexing with SalB, the polar head of phospholipid was

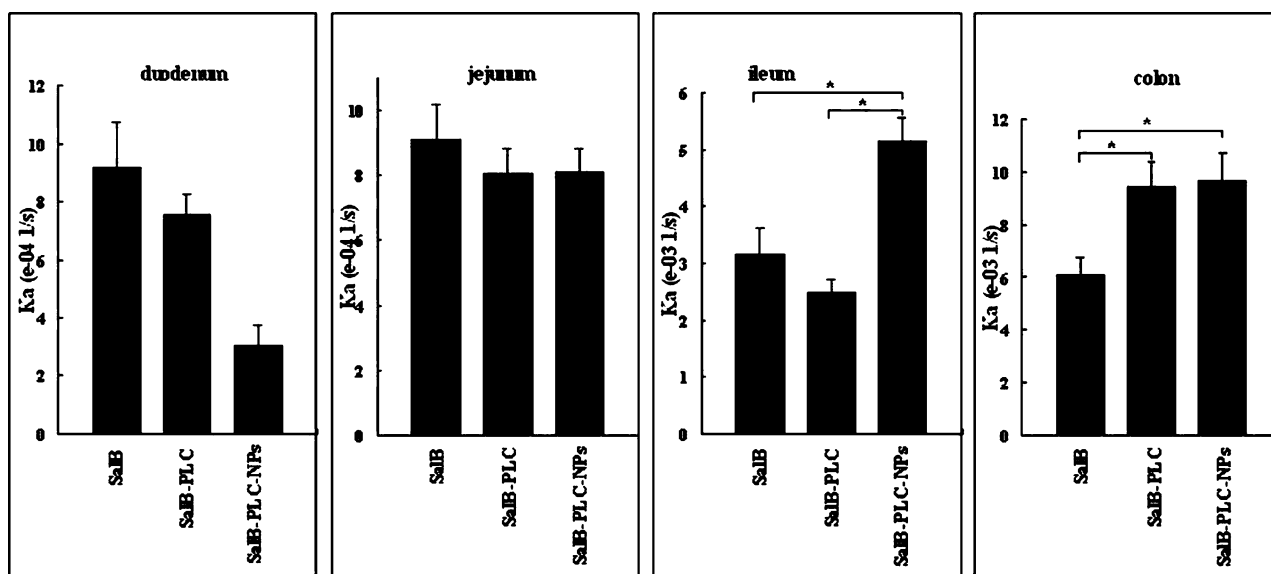


Figure 5. The absorption rate constant (K_a) obtained by in situ perfusion in SPIP model, comparison among three drugs. Data presented as mean \pm SD ($n = 5$). * $P < 0.05$.

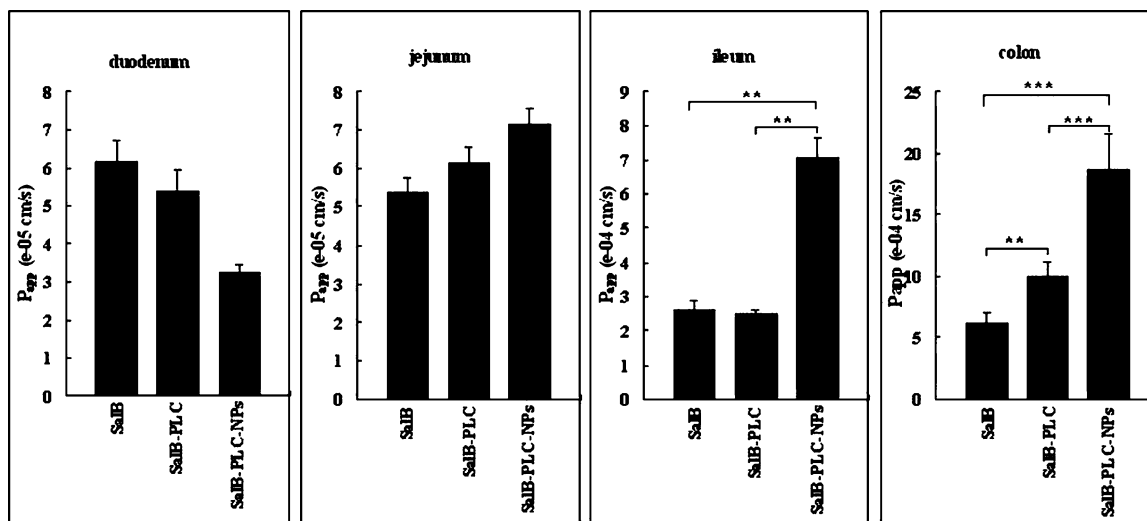


Figure 6. The apparent permeability coefficients (P_{app}) obtained by in situ perfusion in SPIP model, comparison among three drugs. Data presented as mean \pm SD ($n = 5$). ** $P < 0.01$; *** $P < 0.001$.

connected to the phenolic hydroxyl groups of SalB, probably by hydrogen bond.³³ As a result, the complex was highly lipophilic. It was assumed that when SalB-PLC dispersed in organic phase was injected into the aqueous solution, the hydrocarbon tail of complexed phospholipid curved to reduce surface energy, and finally the complex entered the hydrophobic center of free phospholipid to form nanoparticles by emulsification.

The particle size, size distribution and zeta potential have substantial effects on the stability of a nanoparticle system. Nanoparticles prone to aggregate and precipitate if the particle size is large, or the size distribution is not even, or the zeta potential is low. The characteristic of size distribution

is presented by polydispersity index (PDI), the value of which is between 0 and 1; lower value indicates better distribution. In the present work, regardless of the media, the PDI of SalB-PLC-NPs was always lower than 0.200, which might be due to the high pressure homogenization process. The high zeta potential of the produced nanoparticles probably resulted for two reasons. First, to some extent a certain amount of SalB-PLC existing on the surface of nanoparticles would be ionized in nonacidic medium due to the carboxy groups on the SalB molecule. Second, a part of phospholipids would be negatively charged in water solution with neutral pH value, such as phosphatidylserine. In conclusion, the small particle size, low PDI value and high zeta potential indicated the fine stability of the prepared nanoparticle system.

There are several approaches for measuring the entrapment efficiency and drug loading of a nanoparticle system, including Sephadex column filtration, ultracentrifugation,

(33) Venema, F. R.; Weringa, W. D. The interactions of phospholipid vesicles with some anti-inflammatory agents. *J. Colloid Interface Sci.* 1988, 125, 484–500.

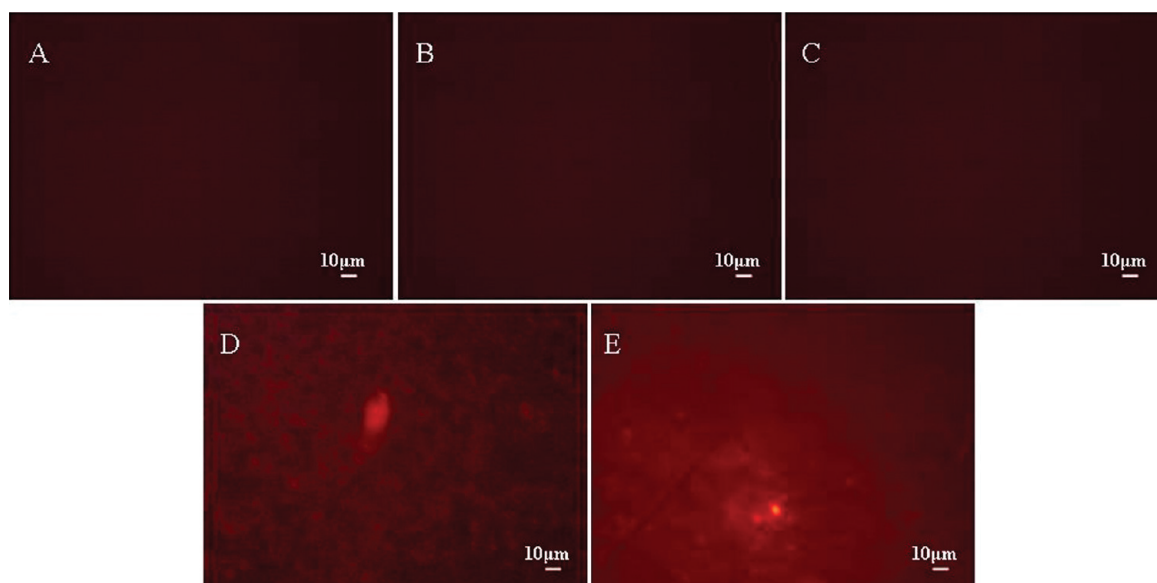


Figure 7. Fluorescent images of lymph taken at 1 h after administration in different intestinal segments. (A) Blank lymph. (B) Lymph sample after duodenum administration. (C) Lymph sample after jejunum administration. (D) Lymph sample after ileum administration. (E) Lymph sample after colon administration.

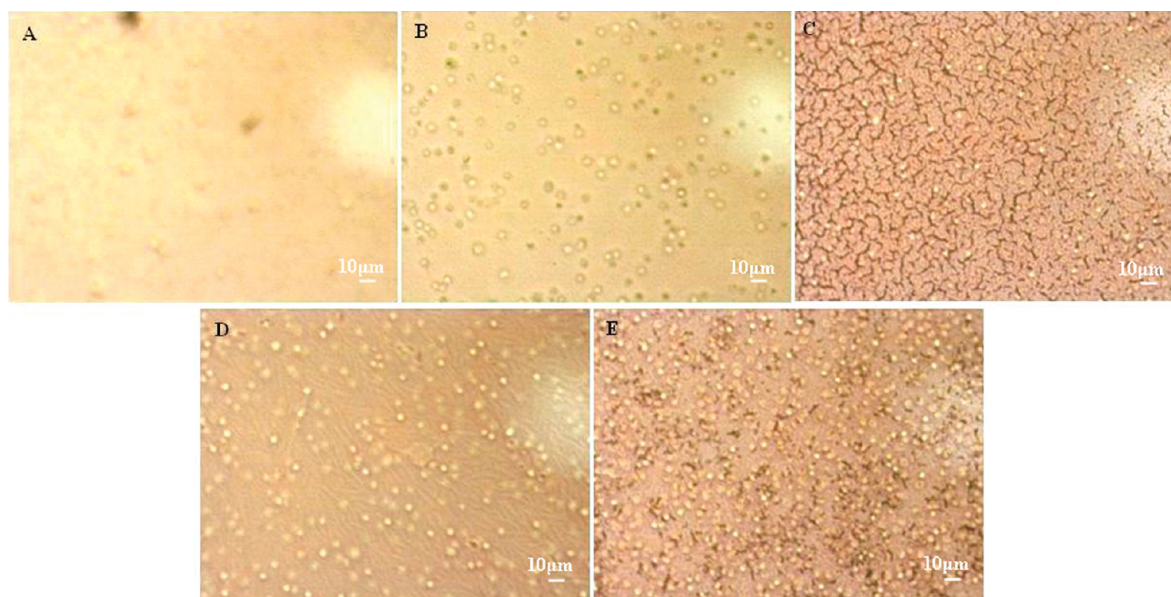


Figure 8. Micrographs of lymph taken at 1 h after administration in different intestinal segments. (A) Blank lymph. (B) Lymph sample after duodenum administration. (C) Lymph sample after jejunum administration. (D) Lymph sample after ileum administration. (E) Lymph sample after colon administration.

dialysis, ultrafiltration, and so on. Among these methods, ultracentrifugation is frequently used due to its convenience. In some cases, however, using ultracentrifugation it is difficult to completely separate free drug from nanoparticles, especially the ones with smaller particle size and higher zeta potential. Hence, some modifications to the traditional method might be necessary.

High negative charge, which played a very important role in enhancing the stability of the nanoparticle system by repelling force, existed on the surface of SalB-PLC-NPs (zeta potential was about -44.2 mV). Therefore, we added 0.1 M HCl to reduce the negative charge of SalB-PLC-NPs. Nanoparticles became aggregated and precipitated when zeta

potential was close to zero, which significantly facilitated the separation of free drug from nanoparticles using ultracentrifugation.

Although the high zeta potential can improve the stability of the nanoparticle system, it is well-known that if nanoparticles were in the state of suspension in aqueous solution for a long term, the system would be destroyed because of oxidation of phospholipid, drug leakage, particle aggregation and bacterial growth. In our study, lyophilization technique was applied to maintain the long term physicochemical stability of the nanoparticle system. Maltose, which served as a cryoprotectant, was used for enhancing the quality of

lyophilized products. As shown in Tables 1 and 2 SalB-PLC-NPs before and after lyophilization presented similar quality. It is notable that, when the lyophilized product was reconstituted in 0.1 M HCl, the zeta potential was inverted to positive charge with lower values, indicating that 0.1 M HCl was able to not only neutralize the negative charge of SalB-PLC-NPs but also make it positively charged. It might be the lower value of positive charge that contributed to a little aggregation of nanoparticles and resulted in the increased particle size. As such it is presumed that SalB-PLC-NPs can maintain relatively stable in the GIT. Overall, the characterization and stability of lyophilized SalB-PLC-NPs in our studies indicated that the lyophilization process developed in the current study was reliable and able to maintain the stability of the nanoparticle system without affecting the quality.

In the in vitro release studies, artificial gastric juice (0.1 M HCl with pH 1.2) and artificial intestinal juice (PBS with pH 6.8 and 7.4) were selected as the dissolution media for SalB-PLC-NPs in response to its oral administration. As seen in Figure 2 the phenomenon of initial burst release in all curves was significantly visible. There might be two factors contributing to the initial burst release. First, the drug which existed on the surface and/or in the surface layer of nanoparticles was easily released into dissolution media. Second, the encapsulated drug was quickly released from matrix through the pores and cracks of nanoparticles.³⁴ It is also clear that the rate of drug release in artificial intestinal juice was much higher than that in artificial gastric juice. It was presumed that phospholipid complex might disintegrate faster in the neutral medium, and SalB molecule would be ionized in intestinal juice with higher pH values, thus facilitating the escape of entrapped drug from nanoparticles, which might also have resulted in the phenomenon that the drug release rate in intestinal juice with pH of 7.4 was a little faster than that in intestinal juice with pH of 6.8.

In the stomach absorption studies, the quite poor absorption of all three drugs was observed, which might be attributed to the smaller absorption area in the stomach. To some extent, the absorption of SalB-PLC and SalB-PLC-NPs in the stomach was higher than that of SalB. It might be attributable to phospholipid that could increase the compatibility between drug and mucous membrane of stomach.

In order to make full use of the intestine length, which would be wasted if only one single segment was perfused, two individual intestinal segments (duodenum, ileum or jejunum, colon) of each rat were simultaneously perfused. The main advantage of this modification was to reduce the number of rats used in the experiments. As presented in Figure 3–6, colon was the best site for absorption of all the three drugs, and only a few amounts of drugs were absorbed in duodenum and jejunum without significant difference. The

good absorption occurred when SalB-PLC-NPs were perfused in ileum ($K_a = 5.14 \pm 0.42 \times 10^{-3}$; $P_{app} = 7.04 \pm 0.62 \times 10^{-4}$) and the best in colon ($K_a = 9.70 \pm 1.02 \times 10^{-3}$; $P_{app} = 1.87 \pm 0.29 \times 10^{-3}$), indicating that ileum and colon were the main absorption sites for nanoparticles. That might be attributed to the fact that there are more Peyer's patches and M-cells in ileum and colon. The most noticeable feature of M-cells was their active transport of a wide variety of inert material from the gut lumen to the follicles (the most obvious component of Peyer's patches), from where particles could migrate to the blood via the mesentery nodes and the thoracic lymph duct.³⁵ SalB-PLC could also be well absorbed in colon ($K_a = 9.43 \pm 0.98 \times 10^{-3}$; $P_{app} = 1.00 \pm 0.12 \times 10^{-3}$). It was assumed that SalB-PLC, as a lipophilic material, might undergo self-aggregation in aqueous media to form spherulike particles due to surface tension, which could also be taken up by M-cells to a certain extent. As such the effect of particle size on the absorption cannot be omitted. According to previous reports by other groups,^{36,37} NPs of ~ 100 nm could be endocytosed by M-cells more efficiently than NPs with larger size. Moreover NPs of ~ 100 nm could also be internalized by normal absorptive enterocytes more readily than larger NPs. After uptake into the enterocyte these smaller NPs might enter the blood circulation either by entering portal blood directly or by intestinal lymphatic transport. Those NPs with size above 500 nm, however, nearly do not enter the systemic circulation. In addition and probably to a small extent, smaller NPs could be absorbed by temporarily opening the epithelial tight junction much more than larger NPs. These reasons might be able to explain why SalB-PLC-NPs showed a better absorption than SalB-PLC.

In recent years the intestinal lymphatic drug transport was increasingly emphasized. The possibility of lymphatic transport of SalB-PLC-NPs was investigated using mesenteric lymph vessel cannulation. The particles observed in Figure 8 were not administered nanoparticles but probably lipoproteins. Nanoparticles might be incorporated into lipoproteins in endochylema after being taken up by intestinal absorptive cells and transported to mesenteric lymph. These results might be able to confirm the transport of SalB-PLC-NPs through the lymph, but the extent of contribution of M-cells to the lymphatic transport was still unknown. The main advantage of intestinal lymphatic drug transport was that drugs absorbed via the intestinal lymphatic system were essentially protected from hepatic first-pass metabolism since the mesenteric lymph, in contrast to the portal blood, entered

(34) Yeo, Y.; Park, K. Control of encapsulation efficiency and initial burst in polymeric microparticle systems. *Arch. Pharm. Res.* **2004**, *27*, 1–12.

(35) Hussain, N.; Jaitley, V.; Florence, A. T. Recent advances in the understanding of uptake of microparticulates across the gastrointestinal lymphatics. *Adv. Drug Delivery Rev.* **2001**, *50*, 107–142.

(36) Jani, P.; Halbert, G. W.; Langridge, J.; Florence, T. The uptake and translocation of latex nanospheres and microspheres after oral administration to rats. *J. Pharm. Pharmacol.* **1989**, *41*, 809–812.

(37) Desai, M. P.; Labhasetwar, V.; Amidon, G. L.; Levy, R. J. Gastrointestinal uptake of biodegradable microparticles: effect of particle size. *Pharm. Res.* **1996**, *13*, 1838–1845.

the systemic circulation directly without first passing through the liver.³⁸ Therefore, intestinal lymphatic transport might have a substantial impact on enhancing drug bioavailability after oral administration, especially for the drugs that would be deactivated by hepatic metabolism.

Conclusion

In conclusion, we have successfully complexed SalB with phospholipid to form SalB-PLC and prepared SalB-PLC-NPs by solvent evaporation method. The lyophilized SalB-PLC-NPs were also prepared with 10% maltose as the cryoprotectant. SalB-PLC-NPs showed a nanometer range in particle size, a spherical structure in shape and a sustained

release profile in vitro. Single pass intestinal perfusion studies showed the segment dependent absorption characteristics of SalB, SalB-PLC and SalB-PLC-NPs. The highest absorption occurred when SalB-PLC-NPs were perfused in colon. Microscope (fluorescence and natural light) observation of lymph indicated that nanoparticles underwent intestinal lymphatic transport. These results suggested that the enhanced oral bioavailability of SalB contributed to both phospholipid complex and nanoparticles. Importantly, PLC-NPs may be a promising delivery system to enhance the oral bioavailability of highly water-soluble drugs.

Acknowledgment. This work was supported by the National Science and Technology Major Project (No. 2009ZX09310-002) of P. R. China and by National Science Foundation (No. 30873165) of P. R. China.

MP900274U

(38) Trevaskis, N. L.; Charman, W. N.; Porter, C. J. H. Lipid-based delivery systems and intestinal lymphatic drug transport: A mechanistic update. *Adv Drug Delivery Rev.* **2008**, *60*, 702–716.